APPLIED PHYSICS LETTERS VOLUME 85, NUMBER 4 26 JULY 2004

Plasma wave detection of sub-terahertz and terahertz radiation by silicon field-effect transistors

W. Knap,[a] F. Teppe, Y. Meziani, N. Dyakonova, and J. Lusakowski
GES CNRS-Universite Montpellier2 34900 Montpellier, France

F. Boeuf and T. Skotnicki
ST Microelectronics, BP 16, 38921 Crolles, France

D. Maude
Grenoble High Magnetic Field Laboratory CNRS-MPI 38 450 Grenoble, France

S. Rumyantsev and M. S. Shur
Center for Broadband Data Transport Science and Technology and Electrical, Computer and System Engineering Department, Rensselaer Polytechnic Institute, Troy, New York 121180-3590

(Received 23 April 2004; accepted 24 May 2004)

We report on experiments on photoresponse to sub-THz (120 GHz) radiation of Si field-effect transistors (FETs) with nanometer and submicron gate lengths at 300 K. The observed photoresponse is in agreement with predictions of the Dyakonov–Shur plasma wave detection theory. This is *experimental evidence of the plasma wave detection by silicon* FETs. The plasma wave parameters deduced from the experiments allow us to predict the nonresonant and resonant detection in THz range by nanometer size silicon devices—operating at room temperature. © *2004 American Institute of Physics*. [DOI: 10.1063/1.1775034]

Terahertz broadband detectors include bolometers,[1–3] pyroelectric detectors, Schottky diodes,[4,5] and photoconductive detectors.[6] Terahertz resonant and nonresonant detection (and emission) using plasmon resonances in two-dimensional electron gas field-effect transistors was predicted in the early 1990's.[7,8] However, experiments demonstrating such detection and emission have been reported only recently. The resonant detection of terahertz radiation by two-dimensional plasma waves was demonstrated in two different types of field effect devices: a commercial field effect transistor[9,10] and a double quantum well field effect transistor.[11] Recently, plasma wave THz emission was also observed from 60-nm gate GaInAs high electron mobility transistors.[12]

All earlier experiments were performed on III–V materials, such as GaAs/AlGaAs, GaInAs/AlGaAs, and GaN/GaAlGaN heterojunctions and mostly at cryogenic temperatures. This letter presents *experimental evidence of plasma wave detection by silicon* field effect transistors (FETs) *working at room temperature* ($\sim$300 K). The results allow us to predict nonresonant and resonant THz range plasma wave detection by Si devices working at 300 K.

The plasma waves in a gated FET channel have a linear dispersion law, $\omega(k)=sk$. Here s is the plasma wave velocity that depends on carrier density, and k is the wave vector. The velocity of the plasma waves, s, is typically on the order of 10^8 cm/s, which is much larger than the drift velocity of the two-dimensional (2D) electrons in the FET channel. This is why the propagation of plasma waves can be used for new regimes of FET operation, with a much higher frequency than for conventional, transit-time limited devices.

A FET, biased by the gate-to-source voltage and subjected to electromagnetic radiation, can develop a constant drain-to-source voltage, which has a resonant dependence on the radiation frequency $f=\omega/2\pi$ with maxima at the plasma oscillation frequencies.[7,13] The plasma wave velocity depends on the carrier density in the channel, n, and the gate to channel capacitance per unit area C, $s=(e^2n/mC)^{1/2}$, where e is the electron charge, and m is the electron effective mass. In the strong inversion region, the carrier density in the channel is related to the gate voltage as $n=CU_0/e$. U_0 is the gate to channel voltage drive/swing that is defined as $U_0=U_g-U_{th}$, where U_g is the gate voltage and U_{th} is the threshold voltage. In this case, the fundamental plasma frequency can be expressed by an approximate relation $f_o=\omega_0/2\pi=(eU_0/m)^{1/2}/4L$. This relation leads to two important consequences: (i) a sufficiently short (submicron) FET can operate as a THz detector, and (ii) the frequency of this detector can be tuned by the gate voltage. The width of the resonance curve is determined by the inverse time of the electron momentum relaxation, $1/\tau$. The dimensionless parameter, which governs the physics of the problem is $\omega_0\tau$. In the regime such that $\omega_0\tau\gg 1$, the FET operates as a resonant detector. When $\omega_0\ll 1$, the plasma oscillations are overdamped, and the FET response is a smooth function of ω as well as of the gate voltage (nonresonant broadband detection). The reduction of τ *at higher temperatures due to enhanced phonon scattering can be alleviated or compensated by increasing* ω_0 via decreasing the device length and/or via increasing the carrier density in the channel.

n-type (MOSFETs) used in our experiments had a 1.2 nm gate oxide, with a 1200 Å N+ polygate. The test structures consisted of transistor arrays with common source and gate contacts and variable gate lengths (ranging from 800 to 30 nm). The gate width, W, was 10 μm.

Figure 1 shows the transistor transfer current–voltage characteristics measured at the drain voltage $V_d=20$ mV corresponding to the linear part of output current–voltage characteristics for all transistors. As seen, all the transistors have approximately the same threshold voltage of $V_t\sim 0.3$ V.

[a]Electronic mail: Knap@univ.montp2.fr

 © 2004 American Institute of Physics

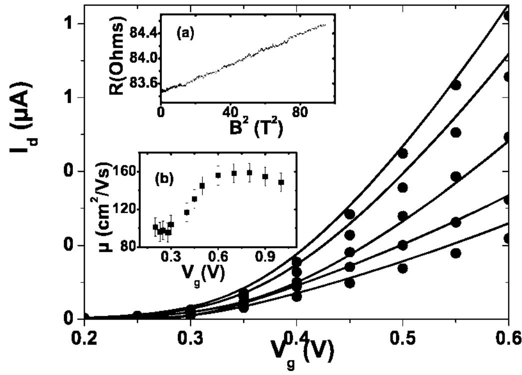

FIG. 1. Transfer characteristics of Si FETs with different gate lengths (800, 600, 100, 40, and 30 nm; the current increases with decreasing gate length). Solid lines show the fits using Eq. (1) and mobility determined from the magnetoresistance experiments. The inset (a) shows the mobility vs gate voltage for an $L_g=100$ nm transistor. Inset (b) shows the source drain resistance vs square of the magnetic field for a transistor with $L_g=40$ nm.

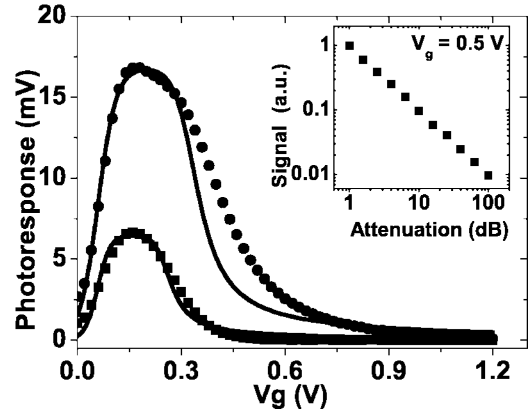

FIG. 2. Detected drain-source signal as a function of the gate voltage for two transistors with 600 nm (squares) and 800 nm (circles) gates. Radiation frequency $f=120$ GHz, $T=300$ K. Inset shows the signal vs attenuation for the gate voltage 0.5 V.

Geometric magnetoresistance measurements[14] in high magnetic fields allowed us to extract the channel mobility μ. The inset (a) in Fig. 1 shows an example of the magnetoresistance measured in magnetic fields up to 10 T. As expected, the resistance increases linearly with B^2:$R=R_0(1+\mu^2B^2)$. The extracted dependence of the mobility on the gate voltage for a 100 nm transistor is shown in Fig. 1(b).

The transfer characteristics were interpreted using the general equation for the electron concentration in a FET channel[15]

$$n=n^{*}\ln\left[1+\exp\left(\frac{eU_0}{\eta k_BT}\right)\right], \quad (1)$$

where $n*=C\eta k_BT/e^2$, C is the gate capacitance per unit area and η is the ideality factor related to the electron density in the subthreshold region. For large positive values of gate voltage

$$\left(U_0>\frac{\eta k_BT}{e}\right)$$

the electron concentration in the FET channel increases with the gate voltage swing as

$$n=\frac{CU_0}{e}.$$

.

The solid lines in Fig. 1 are fits of the transfer characteristics using Eq. (1) and experimentally determined mobility ($\sigma=ne\mu$). The ideality factor η and the threshold voltage were the only fitting parameters, which are listed in Table I.

Using the relaxation time determined from the mobility one can estimate that for frequencies below 1 THz for all our devices the condition $\omega_0\tau\ll 1$ is fulfilled, this means that plasma oscillations are overdamped, and the photoresponse of FET is expected to be a smooth function of ω as well as of the gate voltage (nonresonant broadband detection).

The photoresponse measurements were performed using a 120 GHz back-wave oscillator (BWO) radiation system. The maximum output power was 45 mW. A calibrated power attenuator was used to measure the signal versus output power characteristics.

A waveguide finished with a cone was connected to the output of the BWO to outcouple the radiation. The radiation beam was not focused and the radiation beam diameter at the sample holder was ~10 mm (i.e., much larger than the device size). No special coupling antennas were used and the radiation was coupled to the device through metallization pads.

The radiation intensity was modulated with a mechanical chopper (30–40 Hz range) and the open-circuit source drain voltage was measured using a lock-in technique. The results for 600 and 800 nm devices are shown in Fig. 2. The inset shows the signal versus incoming radiation power dependence measured for gate voltage of 0.5 V. One can observe a very good linearity over two decades.

According to Ref. 10, the photoresponse as a function of the gate voltage is given by:

$$\Delta u=\frac{eu_a^2}{4ms^2}\left\{\frac{1}{1+\kappa\exp\left(-\frac{eU_0}{\eta k_BT}\right)}-\frac{1}{\left[1+\kappa\exp\left(-\frac{eU_0}{\eta k_BT}\right)\right]^2\left[sh^2Q+\cos^2Q\right]}\right\}, \quad (2)$$

where $Q=\sqrt{\omega/2\tau}L/s$, $\kappa=j_0L^2me/2C\tau\eta^2k_B^2T^2$ is a dimensionless parameter related to the leakage current, which is assumed to be small ($\kappa\ll 1$) and s is the plasma wave velocity given by

$$s^2=s_0^2\left[1+\exp\left(-\frac{eU_0}{\eta k_BT}\right)\right]\ln\left[1+\exp\left(\frac{eU_0}{\eta k_BT}\right)\right].$$

The parameters η and U_{th} related to the electron density in the subthreshold region were determined from the transfer characteristics. The relaxation time was taken from the mag-

TABLE I. Parameters of the transistors used in the plasma wave experiments. L_g - gate length, μ - mobility for $V_g=0.4$ V, η- ideality factor, V_{th} - threshold voltage, κ - gate leakage parameter.

L_g(nm)	30	40	600	800
μ(cm^2/V s)	106	119	320	330
η	1.8	1.8	0.7	0.9
V_{th}(V)	0.35	0.35	0.30	0.30
κ	2×10^{-3}	1×10^{-3}	1×10^{-6}	5×10^{-5}

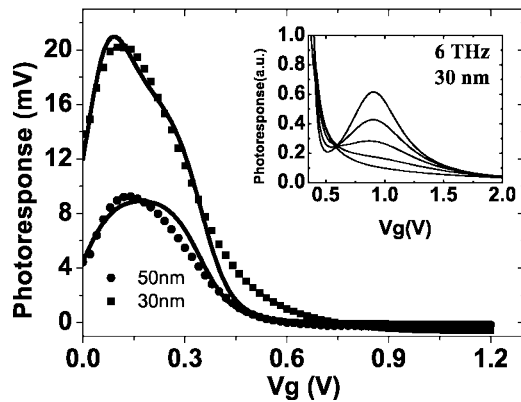

FIG. 3. Detected drain-source signal as a function of the gate voltage for two transistors [30 nm (squares) and 50 nm (circles)]. Radiation frequency $f=119$ GHz. $T=300$ K. The inset shows the calculation of the photoresponse for higher mobilities—with increasing mobility (100 cm^2/V s, 200 cm^2/V s, 300 cm^2/V s, 400 cm^2/V s, 500 cm^2/V s) signal rises and changes from a nonresonant response to a resonant response.

netoresistance mobility measurements. Therefore the parameter kappa—related to the gate leakage current, was the only fitting parameter. The solid lines Fig. 2 are fits of the plasma wave theory[10] to experimental result. As seen, the theory reproduces relatively well the overall shape of the experimental data, including the position and the width of the observed maximum. The discrepancies can be explained by the fact that in the theory the mobility and the gate leakage current are assumed constant. In reality both these parameters depend on the gate voltage. The magnetoresistance measurements show, for example, that the mobility changes by approximately 50% with gate voltage increasing from the subthreshold ($\sim$0.3 V) to the saturation region ($\sim$1 V)—see inset (b) in Fig. 1.

Another explanation of the observed maximum is related to a strong nonuniformity of the carrier distribution in the channel below threshold, when a potential barrier existing between the drain and the source makes the capacitance per unit area very small in its vicinity. Therefore, the differences between the capacitances per unit area at the channel edges become insignificant in comparison, and, the detection responsivity (relying on the asymmetry in the boundary conditions) should decrease precipitously.

Note that the frequency used in these experiments is much higher than the "classical" cutoff frequency for devices with $L > 300$ nm. This result clearly demonstrates the possibility of plasma wave THz operation of these nanometer scale devices.

The photoresponse to 120 GHz radiation was also measured for ultrashort transistors with 30 and 50 nm gates (see Fig. 3). In this case also the plasma wave detection theory (solid lines) reproduces the shape of the observed signals. The calculations based on the extracted parameters (see Table I) predict that a resonant detection for THz frequencies might be possible. Using the theory of the resonant plasma wave detection of Ref. 8, we calculated the photoresponse of a 30 nm FET for frequency 6 THz and mobilities increasing from 100 cm^2/V s to 500 cm^2/V s. The results are shown in the inset of Fig. 3. One can see that a 30 nm FET can reach the resonant THz detection region—a well defined resonant detection can be expected for frequency 6 THz providing the mobility reaches $\sim$300 cm^2/V s. Higher mobility devices (such as strained channel silicon MOSFETs) can reach mobilities of up to a few hundred cm^2/V s and exhibit a resonant detection at lower frequencies.

In conclusion, we have demonstrated the photoresponse to sub-THz/millimeter wave radiation of a gated two-dimensional electron gas in nanometer Si FETs caused by plasma wave detection. *Our results provide experimental evidence of nonlinear plasma wave effects in silicon devices and predict that sub-50* nm *silicon transistors can be used as selective and voltage tunable detectors of THz radiation operating at room temperature.*

The authors thank M. Dyakonov and G. Ghibaudo for helpful discussions and M. Sadowski for critical corrections of the manuscript. We thank also Mr. M. Szot for help in the experiments.

[1]M. Kroug, S. Cherednichenko, H. Merkel, B. Kollberg, B. Voronoy, G. Gol'tsman, H. W. Huebers, H. Richter, IEEE Trans. Appl. Supercond. **11**, 962 (2001).

[2]P. J. Burke, R. J. Schoelkopf, D. E. Prober, A. Skalare, B. S. Karasik, M. C. Gaidis, W. R. McGrath, B. Bumble, and H. G. LeDuc, J. Appl. Phys. **85**, 1644 (1999).

[3]B. S. Karasik, W. R. McGrath, M. E. Gershenson, and A. V. Sergeev, J. Appl. Phys. **87**, 7586 (2000).

[4]T. W. Crow, R. J. Mattauch, R. M. Weikle, U. V. Bhapkar, in *Compound Semiconductor Electronics* (Wor1d Scientific, Singapore, 1996), p. 209.

[5]S. M. Marazita, W. L. Bishop, J. L. Hesler, K. Hui, W. B. Bowen, and T. W. Crowe, IEEE Trans. Electron Devices **47**, 1152 (2000).

[6]J. Q. Wang, P. L. Richards, J. W. Beeman, and E. E. Haller, Appl. Opt. **26**, 4767 (1987).

[7]M. Dyakonov, M. S. Shur, in *Tetrahertz Sources and Systems*, edited by R. E. Miles (Kluwer Academic, Netherlands, 2001), pp. 187–207.

[8]M. Dyakonov and M. S. Shur, Phys. Rev. Lett. **71**, 2465 (1993); M. Dyakonov and M. S. Shur, IEEE Trans. Electron Devices **43**, 380 (1996).

[9]W. Knap, Y. Deng, S. Rumyantsev, and M. S. Shur, Appl. Phys. Lett. **81**, 4637 (2002); W. Knap, Y. Deng, S. Rumyantsev, J.-Q. Lü, M. S. Shur, C. A. Say1or, and L. C. Brunel, *ibid.* **80**, ■ ■(2002).

[10]W Knap, V. Kachorovskii, Y. Deng, S. Rumyantsev, J.-Q. Lü, R. Gaska, M. S. Shur, G. Simin, X. Hu, M. Asif Khan, C. A. Saylor, L. C. Brunel, J. Appl. Phys. **91**, 8436 (2002).

[11]X. G. Peralta, S. J. Allen, and M. C. Wankee, Appl. Phys. Lett. **81**, 1627 (2002).

[12]W. Knap, J. Lusakowski, T. Parenty, S. Bollaert, A. Capy, V. V. Popov, and M. S. Shur, Appl. Phys. Lett. **84**, 3523 (2004).

[13]M. Dyakonov and M. S. Shur, Inst. Phys. Conf. Ser. **145**, 785 (1996), Chapter 5.

[14]Y. M. Meziani, J. Lusakowski, W. Knap, N. Dyakonova, F. Teppe, K. Romanjek, M. Ferrier, R. Clerc, G. Ghibaudo, F. Boeuf, and T. Skotnicki (unpublished).

[15]T. Fjeldly, T. Ytterdal, and M . S. Shur, *Introduction to Device and Circuit Modeling for VLSI* (Wiley, New York, 1998); M. S. Shur, *Introduction to Electronic Devices* (Wiley, New York, 1996).